

# Reversal effect of adenovirus-mediated human interleukin 24 transfection on the cisplatin resistance of A549/DDP lung cancer cells

MINGJU XU<sup>1</sup>, XIOAWEI TANG<sup>2</sup>, JINJIN GUO<sup>3</sup>, WANGBANG SUN<sup>3</sup> and FAQING TANG<sup>1</sup>

<sup>1</sup>Department of Clinical Laboratory of Zhuhai Hospital, Jinan University and Zhuhai People's Hospital, Zhuhai, Guangdong 519000; <sup>2</sup>Metallurgical Science and Engineering, Central South University, Changsha, Hunan 410083; <sup>3</sup>Zhuhai Campus, Zunyi Medical College, Zhuhai, Guangdong 519041, P.R. China

Received February 24, 2017; Accepted September 18, 2017

DOI: 10.3892/or.2017.6002

**Abstract.** Interleukin-24 (IL-24) is a tumor-suppressor gene that has been documented in human melanoma cells. IL-24 has marked antitumor activities on various types of human cancer, but its underlying mechanism remains unclear. In the present, we investigated the effects of human IL-24 (hIL-24) on the chemotherapy resistance of lung cancer cells. The cisplatin (DDP)-resistant lung carcinoma cell line A549/DDP was subjected to adenovirus-mediated transfection with the human IL-24 gene (Ad-hIL-24). The growth-inhibitory and apoptotic effects of Ad-hIL-24 on A549/DDP cells were observed, and the expression levels of AKT, phosphorylated-AKT (p-AKT) and P-glycoprotein (P-gp) were detected. Ad-hIL-24 significantly decreased the levels of p-AKT and P-gp, and effectively inhibited A549/DDP cell growth. Furthermore, A549/DDP cells exhibited a significantly increased rate of apoptosis, as well as G2/M-phase arrest, following transfection with Ad-hIL-24, and these effects were increased in cells treated with Ad-IL-24 combined with DDP when compared with those treated with Ad-hIL-24 or DDP alone. These results suggest that hIL-24 can reverse the DDP resistance of lung cancer cells, and that the associated mechanism involves the induction of apoptosis and G2/M-phase arrest through the

phosphoinositide3-kinase (PI3K)/AKT signaling pathway, as well as a decrease in drug resistance through P-gp expression.

## Introduction

Lung cancer is a common malignant tumor worldwide, and its incidence and mortality rates have significantly increased in recent years (1,2). Since the clinical manifestations of early lung cancer are often hidden and lack specificity, most patients are not diagnosed until the disease has reached an advanced stage (3). At present, for patients with late-stage lung cancer, the main treatment strategy is chemotherapy or chemotherapy combined with radiotherapy (4,5). Chemotherapy can kill tumor cells, but it can also exert strong side effects on normal cells (6). Furthermore, after multiple cycles of chemotherapy, tumor cells can develop resistance to chemotherapeutic drugs. Multidrug resistance (MDR) is the acquired resistance of cancer cells to structurally and functionally different chemotherapeutic drugs (7), and remains a major obstacle to chemotherapy efficacy, decreasing the effectiveness of treatment for patients with lung cancer (8,9). Thus, it is important to investigate the mechanisms related to MDR and to improve the efficacy of chemotherapy for lung cancer.

Many studies have shown that the MDR mechanism of tumors is mainly related to the ATP-binding cassette (ABC) transporter superfamily of genes, such as P-glycoprotein (P-gp; encoded by the MDR1 gene), which code for efflux pump proteins (10,11). P-gp overexpression can increase the rate at which drugs are pumped out of cells, which reduces the chemotherapeutic effects of the drugs, inducing drug resistance (12,13). Furthermore, tumor MDR mechanisms are associated with detoxification, repair and various signal transduction pathways (14). Generally, the drug resistance mechanisms in lung cancer are complex, involving many factors; therefore, it is considered highly important to identify efficient, low-toxicity methods of reversing lung cancer MDR.

Gene therapy has introduced new prospects for the treatment of drug resistance in cancer. Interleukin 24 (IL-24), a newly identified antitumor gene, can inhibit the growth of tumor cells, including lung, breast and ovarian cancer cells, and is considered to be combinable with radiotherapy

---

*Correspondence to:* Dr Faqing Tang, Department of Clinical Laboratory of Zhuhai Hospital, Jinan University and Zhuhai People's Hospital, 79 Kangning Road, Zhuhai, Guangdong 519000, Guangdong, P.R. China  
E-mail: tangfaqing33@hotmail.com

*Abbreviations:* Ad-GFP, Ad-green fluorescent protein; Ad-hIL-24, adenovirus-mediated human interleukin 24 gene; CCK-8, Cell Counting Kit-8; DDP, cisplatin; hIL-24, human interleukin-24; HRP, horseradish peroxidase; IC<sub>50</sub>, half maximal inhibitory concentration; MDR, multidrug resistance; MOI, multiplicity of infection; PBS, phosphate-buffered saline; p-AKT, phosphorylated-AKT; P-gp, P-glycoprotein; PI3k, phosphoinositide-3-kinase; PMSF, phenylmethanesulfonyl fluoride; TBS, Tween-20 phosphate-buffered saline

*Key words:* interleukin 24, lung cancer, drug resistance, AKT, P-gp

or chemotherapy, which could improve the effects of radiotherapy and chemotherapy on tumor cells (15-17). The IL-24 gene has been widely investigated in various cancers for its role as a tumor-suppressor gene, particularly with regard to tumor gene therapy (18); however, its role in reversing MDR has not been investigated in detail. In the present study, we used adenovirus-mediated human IL-24 gene (Ad-hIL-24) transfection and the cisplatin (DDP)-resistant human lung adenocarcinoma cell line A549/DDP to study whether IL-24 can reverse the MDR of lung cancer as well as investigate its mechanism. The results revealed that Ad-hIL-24 could effectively increase the anticancer effect of DDP on A549/DDP cells and induce A549/DDP cell apoptosis. These effects were associated with decreases in the expression levels of phosphorylated AKT (p-AKT) and P-gp.

## Materials and methods

**Adenoviral vectors, cell lines and cell culture.** The DDP-resistant human lung adenocarcinoma cell line A549/DDP (19) was obtained from the Central Laboratory of Xiangya Medical College of Central South University (Hunan, China). Ad-hIL-24, an adenoviral vector containing the hIL-24 gene, which is able to effectively express hIL-24 (20), was acquired from the Laboratory of Cell and Molecular Biology, Medicine College, Soochow University (Suzhou, China). QBI-293A (a human embryonic kidney cell line) was provided by Dr Jicheng Yang of Soochow University (Suzhou, China). The cells were cultured in RPMI-1640 (Hyclone, Nanjing, China), supplemented with 10% fetal bovine serum (FBS) (Hyclone). An IL-24 enzyme-linked immunosorbent assay (ELISA) kit was purchased from CusaBiol (Carlsbad, CA, USA; cat. #ELH-IL-24-1). Rabbit anti-human P-gp (#129450), p-Akt (#4060), and Akt (#9272) were purchased from Cell Signaling Technology (Shanghai, China). Antibodies against GAPDH (#ab153802) and IL-24 (#ab182567) were purchased from Abcam (Shanghai, China). The Cell Counting Kit-8 (CCK-8) assay was purchased from Dojindo (Nanjing, China).

**Amplification of Ad-hIL-24 and determination of the rate of infection.** Ad-hIL-24 or Ad-green fluorescent protein (Ad-GFP) were inoculated into QBI-293A cells for the amplification of recombinant adenovirus. When 293A cells became rounded and formed aggregates under microscopy, the cells were considered to be infected by adenovirus, and these cells were collected and centrifuged. The supernatants were subjected to the same step at least three times and then collected. The Ad-hIL-24 or Ad-GFP adenoviruses were diluted to  $10^{-4}$ ,  $10^{-5}$ ,  $10^{-6}$ ,  $10^{-7}$  and  $10^{-8}$ , dispensed into 96-well culture plates, and incubated at 37°C in the presence of 5% CO<sub>2</sub> for 24 h. Following incubation, the fluorescent cells were counted under a fluorescence microscope, and the infection rate and adenoviral titer were calculated. A549/DDP cells were infected with Ad-hIL-24 and Ad-GFP at various multiplicities of infection (MOIs; 25, 50, 100, 150 and 200). GFP expression and infection efficiency were determined under fluorescence microscopy to select the optimal MOI for maximal transgene expression.

**CCK-8 assay.** The viability of treated cells was determined by CCK-8 assay (21). Cells ( $1 \times 10^3$ ) in the logarithmic phase of

growth were inoculated into 96-well plates in 100- $\mu$ l aliquots and incubated at 37°C. Following incubation, 10  $\mu$ l of CCK-8 assay solution (Dojindo) was added to each well. The blank wells contained saline. The absorbance value (A value) for each well was measured at 450 nm with a microplate reader. The cell growth trend was observed by plotting a growth curve, taking the A value as the vertical coordinate and the culture time as the horizontal coordinate. After incubation for 24 h, the cells were treated with 100  $\mu$ l DDP at 5, 10, 25 or 50  $\mu$ g/ml, followed by the addition of 10  $\mu$ l CCK-8 assay solution, and then the value of the cells in each well was assessed. SPSS 17.0 software was used to calculate the DDP dose effect on A549/DDP cells, by using the linear regression equation:  $Y = a + bX$  (where Y represents the DDP dose, and X represents the inhibition rate). The half maximal inhibitory concentration (IC<sub>50</sub>), defined as the dose of drugs to induce 50% inhibition (cellular death) was calculated, and this dose was used in subsequent experiments. In the same way, A549/DDP cells were treated with Ad-GFP, DDP, Ad-hIL-24, or Ad-hIL-24 plus DDP (A549/DDP cells were infected with adenovirus using the aforementioned method, and the MOI and DDP dose were calculated according to the IC<sub>50</sub> value). According to the formula, the required amount of virus (ML) = (MOI x tumor cell number)/viral titer. Saline was used as a negative control. The inhibition rate of A549/DDP cells was counted using the following formula: inhibition rate (%) = (A value of the control - A value of the experimental group)/A value of the control x 100%.

**ELISA assay.** The treated cells were cultured with FBS-free medium for 72 h, and the cell media were then harvested for use in the IL-24 assay with the IL-24 ELISA kit. Briefly, 100  $\mu$ l of culture medium was added to each ELISA well and incubated for 2 h at 37°C. After incubation, the liquid was removed, and 100  $\mu$ l biotin-conjugated antibody was added and incubated for 1 h at 37°C. The supernatant was aspirated and three washes were performed. After the final wash, the remaining liquid was completely removed by aspiration or decanting. The plate was then inverted and blotted against clean paper towels. Into each well, 100  $\mu$ l horseradish peroxidase (HRP)-avidin was added, and incubated for 1 h at 37°C, before the aspiration/wash process was repeated. TMB substrate (90  $\mu$ l) was next added into each well and incubated for 15-30 min at 37°C, prior to the addition of 50  $\mu$ l Stop Solution. The optical density in each well was determined using a microplate reader at 450 nm.

**Western blotting.** Akt, p-Akt, and P-gp expression in the treated A549/DDP cells were detected as previously described with some modifications (22). Briefly, A549/DDP cells were treated with Ad-GFP, Ad-hIL-24, DDP, or Ad-hIL-24 plus DDP for 24 h. The treated cells were collected, and the cellular protein was extracted and assessed by BCA protein assay. Total protein (~100  $\mu$ g) was then loaded into each lane of an acrylamide gel and subjected to SDS-PAGE. Following electrophoresis, the proteins were transferred onto a PVDF membrane, and the membrane was blocked by incubation in 5% non-fat dry milk in 0.1% Tween-20 phosphate-buffered saline (PBS-T) for 1 h at room temperature. The membranes were incubated with antibodies against Akt, p-Akt or P-gp at

4°C overnight. After being washed with PBS-T, the membranes were incubated with HRP-conjugated secondary antibodies for 1 h. The membranes were washed and then developed with a Super enhanced chemiluminescence detection kit. A gel imaging system was used to analyze the gray value of each protein band. The relative photographic density was quantified. GAPDH was used as an internal control to verify the basal expression level and equal protein loading. The abundance ratio relative to GAPDH was determined.

**Hoechst 33342 staining.** Hoechst 33342 staining (Sigma-Aldrich, Shanghai, China) was used to observe the nuclei of A549/DDP cells. Initially, a moderate density of A549/DDP cells was added to each well of a 6-well plate. After incubation for 24 h, the cell wells were treated with Ad-GFP, Ad-hIL-24, DDP, or DDP plus Ad-hIL-24 for 48 h, while the cell medium alone was added to serve as a negative control group. According to the instructions of the Hoechst 33342 kit, the treated cells were washed with PBS and fixed with 4% paraformaldehyde at room temperature for 15 min. The cells were then incubated with Hoechst 33342 (0.5 g/ml) for 15 min. After removing the staining solution from the wells, the cells were washed. The stained nuclei were observed by fluorescence microscopy.

**Flow cytometry.** Cell apoptosis was detected by flow cytometry. The treated cells were stained using Annexin V-fluorescein isothiocyanate (FITC)/propidium iodide (PI), according to the instructions of the Annexin V kit. Briefly, A549/DDP cells ( $5 \times 10^6$ ) were transfected with Ad-GFP, Ad-hIL-24, DDP, or DDP plus Ad-hIL-24, and incubated for 48 h. After incubation, the treated cells were collected and washed with cold PBS. Annexin V-FITC (5  $\mu$ l) and binding buffer (500  $\mu$ l) were added to the cells and incubated for 15 min at room temperature. After incubation, the cells were analyzed by flow cytometry.

**Cell cycle analysis.** A549/DDP cells were treated with Ad-GFP, DDP, Ad-hIL-24, or Ad-hIL-24 plus DDP for 24 h. The treated cells were collected, and subjected to cell cycle analysis as previously described (23). Briefly,  $1 \times 10^4$  A549/DDP cells were seeded into 6-well plates at 30% confluence. After being treated with Ad-hIL-24, the cells were collected, and then incubated overnight with pre-cooled 70% ethanol. The cells were washed once with PBS and then incubated with PI for 15 min for cell cycle analysis after filtering through a 400-micron mesh sieve. The cell samples were then subjected to flow cytometry.

**Statistical analysis.** Data are presented as the mean  $\pm$  standard deviation (SD). More than two groups were compared using a single-factor analysis of variance method.  $P < 0.05$  was considered to indicate statistical significance.

## Results

**Ad-hIL-24 amplification and infected rate in A549/DDP cells.** QBI-293A cells were infected with Ad-hIL-24 or Ad-GFP for 48 h to amplify the vectors. When viewed under an inverted microscope, the infected cells appeared round or flaky, or formed grape-like aggregates. After infection with Ad-GFP,

many fluorescent cells (those infected with recombinant adenovirus) were observed under the fluorescence microscope. QBI-293A cells were repeatedly infected to determine the viral titer up to  $10^8$  pfu/ml. A549/DDP cells were infected with Ad-hIL-24 or Ad-GFP at various MOIs (25, 50, 100, 150 or 200 MOI) for 48 h. Considering that a high rate of infection and low cytotoxicity offers the best MOI, in this study we selected 100 as the optimal MOI for infecting cells. A549/DDP cells were infected with Ad-hIL-24 and Ad-GFP, and the infected cells were counted under a fluorescence microscope (Fig. 1A) to determine the infection rates. The infection rates were  $79.3 \pm 3.7\%$  at 24 h, and  $93.2 \pm 5.6\%$  at 48 h (Fig. 1B).

**Inhibitory effect of Ad-hIL-24 on A549/DDP cell growth.** A549/DDP cells are tolerant to DDP. A549/DDP cells were treated with DDP, Ad-hIL-24, or Ad-hIL-24 plus DDP, and hIL-24 expression levels were detected in the treated cells. hIL-24 was effectively expressed in the cells transfected with Ad-hIL-24 (Fig. 2A), and a high concentration of hIL-24 was detected in the cell media from the Ad-hIL-24 treatment group (Fig. 2B). A549/DDP cells were treated with DDP at various concentrations, and then the viability of the treated cells was detected using the CCK-8 assay. Using the linear regression equation  $y = 45.611x - 0.643$ , the  $IC_{50}$  value of DDP in A549/DDP cells was calculated. The results revealed that A549/DDP cells displayed a high resistance to DDP ( $IC_{50}$ , 22.0  $\mu$ g/ml). This concentration was used as the optimal dose of DDP in subsequent experiments.

To observe the effect of Ad-hIL-24 on A549/DDP cell growth, A549/DDP cells were treated with Ad-hIL-24 for 12, 24, and 48 h, and then the viability of the infected cells was detected using the CCK-8 assay. A549/DDP cell viability was markedly decreased after infection with Ad-hIL-24 (Fig. 2C), and was found to gradually decrease with increasing infection time, especially at 48 h after infection. The viability of these cells was significantly decreased compared with the blank control (Fig. 2C). Furthermore, cell viability was lower in the Ad-hIL-24 plus DDP group than in the groups treated with Ad-hIL-24 or DDP alone (Fig. 2C). This indicated that Ad-hIL-24 could increase the extent of inhibition exerted by DDP on A549/DDP cell viability.

**Inhibition rates of Ad-hIL-24 in A549/DDP cells.** A549/DDP cells were infected with Ad-hIL-24 at 100 MOI and treated with 22.0  $\mu$ g/ml DDP for 12, 24 or 48 h. hIL-24 expression was detected by western-blotting. hIL-24 expression in the Ad-hIL-24 plus DDP group was lower than that in the Ad-hIL-24 group (Fig. 2A and B). In the group of A549/DDP cells treated with DDP alone, hIL-24 expression was not significantly different compared with the control. However, when DDP was combined with Ad-hIL-24 treatment, hIL-24 expression was markedly decreased (Fig. 2A and B). This revealed that there may be a synergistic reaction between Ad-hIL-24 and DDP. The cell viability was detected using a CCK-8 assay. Following a 24-h infection, the inhibitory rates in the Ad-hIL-24, DDP, and Ad-hIL-24 plus DDP groups were  $17.63 \pm 1.55\%$ ,  $11.57 \pm 1.92\%$ ,  $30.03 \pm 1.01\%$ , respectively, which were high compared with that in the control group ( $6.67 \pm 1.34\%$ ;  $P < 0.05$ ; Fig. 2D). After a 48-h infection, the inhibitory rates were  $27.00 \pm 2.00\%$ ,  $19.37 \pm 1.70\%$ , and  $42.93 \pm 2.59\%$ , respectively, which were significantly higher

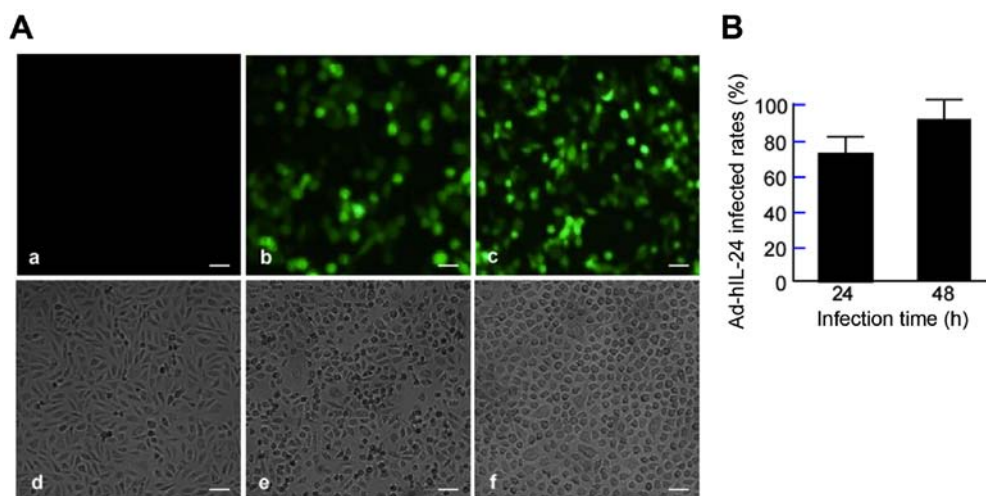


Figure 1. Adenovirus-mediated human interleukin 24 gene (Ad-hIL-24) infects A549/DDP cells. A549/DDP cells were infected with Ad-hIL-24 and Ad-GFP, and incubated for 24 or 48 h. Ad-GFP served as an internal control. The treated cells were fixed with paraformaldehyde and stained with a fluorescent antibody. Saline (DDP solvent) served as the blank controls. (A) Green fluorescent protein (GFP) expression was observed under fluorescence microscopy. Scale bar, 25  $\mu$ m. Magnification,  $\times 100$ . Upper panel, fluorescence microscopy images: a, saline; b, cells infected with Ad-hIL-24 for 24 h; c, cells infected with Ad-hIL-24 for 48 h; Lower panel, light-field images: d, saline; e, cells infected with Ad-hIL-24 for 24 h; f, cells infected with Ad-hIL-24 for 48 h. (B) GFP cells were counted under fluorescence microscopy, and the infected rates were assessed.

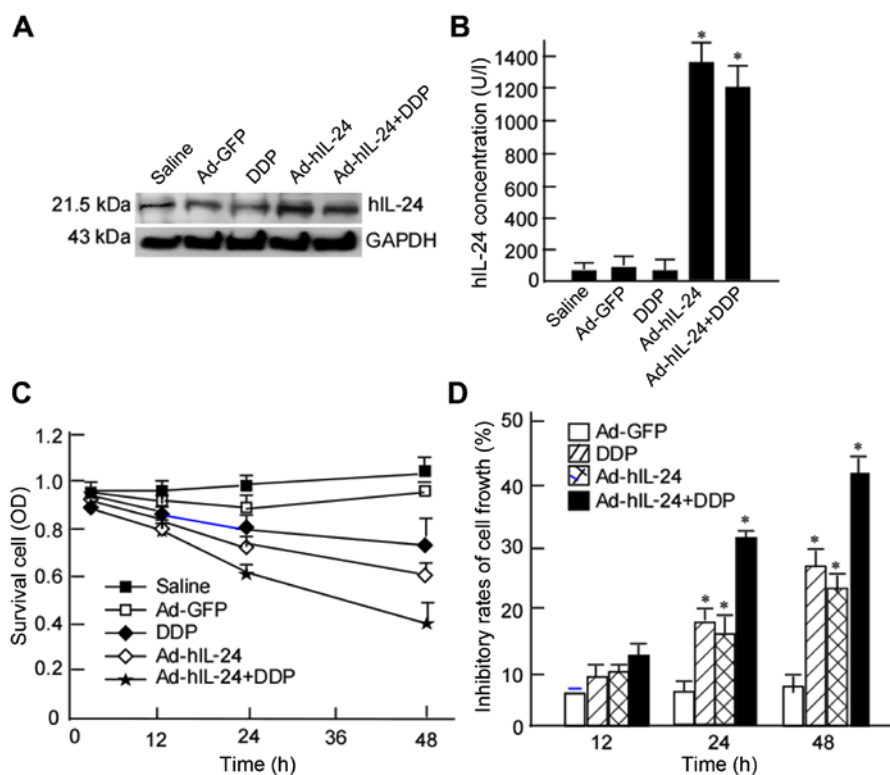


Figure 2. hIL-24 expression and the growth curve of A549/DDP cells infected with Ad-hIL-24. A549/DDP cells were treated with DDP, Ad-hIL-24, and Ad-hIL-24 plus DDP, and then incubated for 48 h. Saline (DDP solvent) served as blank controls and Ad-GFP served as the vector control. (A) hIL-24 expression was detected in the infected cells using western-blotting. (B) The media of the infected cells were harvested, and hIL-24 was detected using ELISA. (C) The cell viability of the infected cells was detected using CCK-8 assay. (D) The inhibitory rates were assessed. Data are presented as the means  $\pm$  SD from three independent experiments statistically using the Student's *t* test ( $P < 0.05$ ).

than that in the control group ( $7.27 \pm 1.93\%$ ;  $P < 0.05$ ; Fig. 2D). The inhibitory rates were also higher at 48 h than at 24 h ( $P < 0.05$ ). This indicated that the inhibition rate was time-dependent, increasing with the increasing reaction time of Ad-hIL-24. The inhibitory rate of the combined treatment group ( $42.93 \pm 2.59\%$ ) was significantly higher than that of the groups treated with

Ad-hIL-24 alone ( $27.00 \pm 2.00\%$ ) or DDP alone ( $19.37 \pm 1.70\%$ ;  $P < 0.05$ ; Fig. 2D). The inhibitory rate increased from 19.37% in the DDP group to 42.93% in the combined group, amounting to a 2.22-times increase in growth inhibition ( $P < 0.05$ ; Fig. 2D). These results indicated that Ad-hIL-24 significantly enhanced the inhibition of A549/DDP cell viability by DDP.

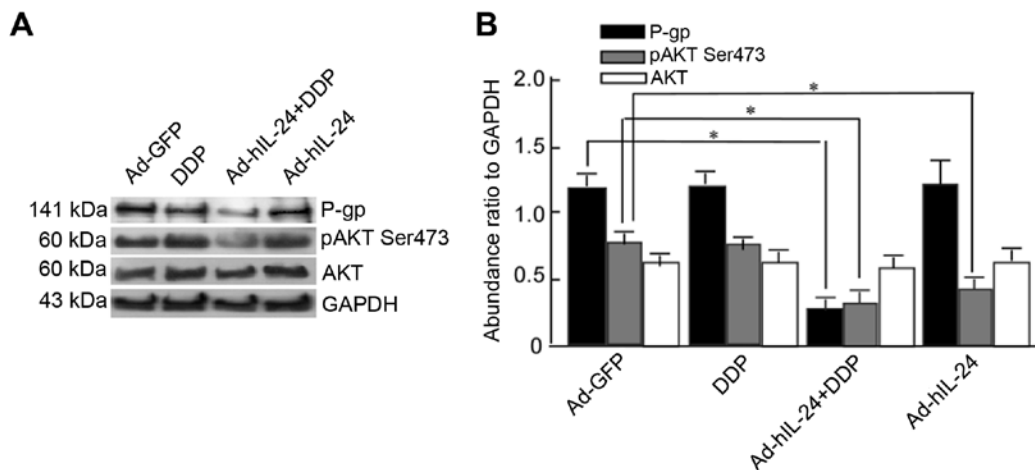


Figure 3. P-gp, AKT and p-AKT expression in A549/DDP cells transfected with Ad-hIL-24. A549/DDP cells were treated with DDP, Ad-hIL-24, and Ad-hIL-24 plus DDP, and incubated for 48 h. Ad-GFP served as the vector control. Total proteins in the treated cells were extracted. The protein samples were subjected to western-blotting. (A) P-gp, AKT and p-AKT expression was detected in the treated cells with DDP, Ad-hIL-24 or Ad-hIL-24 plus DDP. (B) The relative photographic density was quantitated. GAPDH was used as an internal control to ascertain basal level expression and equal protein loading. The abundance ratio relative to GAPDH was counted. Data are presented as the mean  $\pm$  SD from three independent experiments statistically using the Student's t test ( $P < 0.05$ ).

*hIL-24 induces decreases in p-Akt and P-gp expression levels.* hIL-24 may exert a reversal effect on drug resistance in A549/DDP cells. P-gp pumps drugs out of cancer cells, and decreases the effect of chemotherapeutic drugs, thereby rendering cells drug-resistant (6,7). To further investigate whether the effect of hIL-24 was associated with P-gp, A549/DDP cells were treated with Ad-hIL-24, DDP, or Ad-hIL-24 plus DDP, and P-gp expression was detected by western-blotting. P-gp expression was markedly decreased in the combined group when compared with the groups treated with Ad-hIL-24 or DDP alone (Fig. 3A and B;  $P < 0.05$ ). This suggested that Ad-hIL-24 combined with DDP could effectively decrease P-gp expression, and that Ad-hIL-24-mediated growth inhibition may be associated with decreasing P-gp expression. Components of the phosphoinositide-3-kinase (PI3K)/AKT signaling pathway are overexpressed in many tumors; when PI3K is activated, PIP2 and PIP3 expression levels increase and they bind to AKT through their pleckstrin homology (PH) domains, leading to AKT phosphorylation. p-Akt inhibits antiapoptotic signals and promotes cell apoptosis. Thus, we detected p-AKT expression in the treated cells, and obtained the expected results. P-gp and p-Akt expression in the Ad-hIL-24 plus DDP group were significantly decreased when compared with the DDP or Ad-hIL-24 groups (Fig. 3A and B;  $P < 0.05$ ). However, the expression of total Akt was not significantly different among the groups (Fig. 3A and B). This indicated that Ad-hIL-24 plus DDP decreased p-AKT expression, and implied that the role of Ad-hIL-24 in DDP-mediated apoptosis was directly related to decreased p-AKT expression.

*Morphological changes of A549/DDP cells with Ad-hIL-24 treatment.* The aforementioned results showed that Ad-hIL-24 decreased p-AKT expression. p-AKT downregulation has been shown to induce cell apoptosis (24). We next observed the morphological changes in A549/DDP cells following Ad-hIL-24 treatment. A549/DDP cells were treated with Ad-hIL-24, DDP, or Ad-hIL-24 plus DDP for 48 h, then stained

with Hoechst 33342. The morphology of the treated cells was observed under a fluorescence microscope. After treatment, the cell fluorescence intensity increased and some were evenly stained, indicating that the cells had begun to undergo apoptosis (Fig. 4A). In the combined treatment group, a large number of apoptotic cells were present (Fig. 4A-e); the number of apoptotic cells was greater than that in the Ad-hIL-24 (Fig. 4A-c) and DDP alone treatment groups (Fig. 4A-d).

Apoptotic cells were counted under a fluorescence microscope, and the apoptosis rate was calculated. The apoptosis rates of the Ad-hIL-24, DDP, and Ad-hIL-24 plus DDP groups were respectively  $17.50 \pm 1.32\%$ ,  $12.83 \pm 1.04\%$  and  $24.50 \pm 1.00\%$ , all of which were higher than that of the control ( $P < 0.05$ ) (Fig. 4B). The apoptotic rate of the combined group ( $24.50 \pm 1.00\%$ ) was higher than that of the Ad-hIL-24 ( $17.50 \pm 1.32\%$ ) and DDP ( $12.83 \pm 1.04\%$ ) groups ( $P < 0.05$ ). This implied that Ad-hIL-24 increased the apoptosis-inducing effect of DDP on A549/DDP cells.

*Flow cytometric analysis of hIL-24-mediated apoptosis.* To further confirm that hIL-24 enhanced DDP-mediated cell apoptosis, flow cytometry was used to detect the apoptosis of cells treated with Ad-hIL-24, DDP, or Ad-hIL-24 plus DDP. Apoptotic cells were observed in the Ad-hIL-24 plus DDP groups, and were more frequent in these groups than in the control group (Fig. 5A). The flow cytometry data revealed that the apoptosis rates in the groups treated with Ad-hIL-24, DDP, and Ad-hIL-24 plus DDP were  $27.90 \pm 0.98\%$ ,  $16.40 \pm 0.95\%$  and  $39.61 \pm 1.38\%$ , respectively, which were higher than that of the blank and vector control groups ( $7.62 \pm 0.85\%$ ,  $8.25 \pm 1.51\%$ ). The rate of apoptosis in the combined group ( $39.61 \pm 1.38\%$ ) was obviously increased when compared with the groups treated with Ad-hIL-24 ( $27.90 \pm 0.98\%$ ) or DDP alone ( $16.40 \pm 0.95\%$ ) ( $P < 0.05$ ) (Fig. 5B). Those results revealed that Ad-hIL-24 enhances the DDP-induced apoptosis of A549/DDP cells.

*hIL-24 induces A549/DDP cell-cycle arrest.* The aforementioned results revealed that Ad-hIL-24 decreased p-AKT

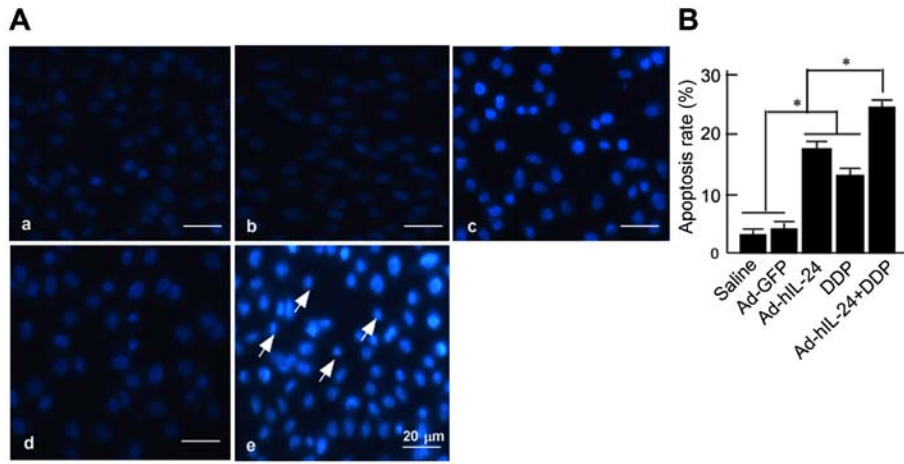


Figure 4. Morphological analysis of Ad-hIL-24-mediated A549/DDP cell apoptosis. A549/DDP cells were treated with DDP, Ad-hIL-24, and Ad-hIL-24 plus DDP, and incubated for 48 h. The treated cells were fixed with paraformaldehyde and then stained with Hoechst 33342. Saline served as the blank control, and Ad-GFP as the vector control. (A) The apoptotic cells were observed under fluorescence microscopy: a, saline; b, Ad-vector; c, Ad-hIL-24; d, DDP; e, Ad-hIL-24 plus DDP. Scale bar, 50  $\mu$ m. Magnification, x400. (B) The rates of apoptotic cells were counted. Data are presented as the means  $\pm$  SD from three independent experiments statistically using the Student's t test ( $P < 0.05$ ).

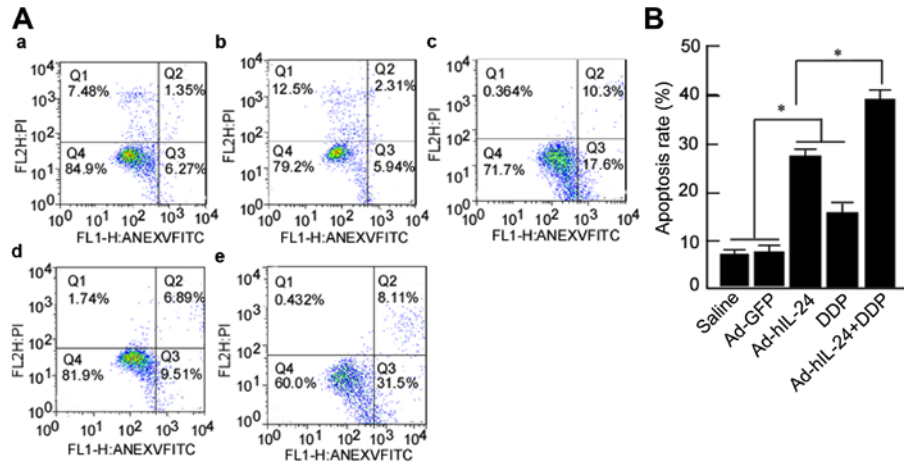


Figure 5. Flow cytometric analysis of Ad-hIL-24-mediated A549/DDP cell apoptosis. A549/DDP cells were treated with DDP, Ad-hIL-24, and Ad-hIL-24 plus DDP, and incubated for 48 h. Then the treated cells were fixed with ethanol and stained with Annexin V-FITC. Saline served as the blank control, and Ad-GFP as the vector control. (A) The apoptotic cells were analyzed with flow cytometry: a, saline; b, Ad-vector; c, Ad-hIL-24; d, DDP; e, Ad-hIL-24 plus DDP. Scale bar, 50  $\mu$ m. Magnification x400. (B) The rates of apoptotic cells were counted. Data are presented as the means  $\pm$  SD from three independent experiments statistically using the Student's t test ( $P < 0.05$ ).

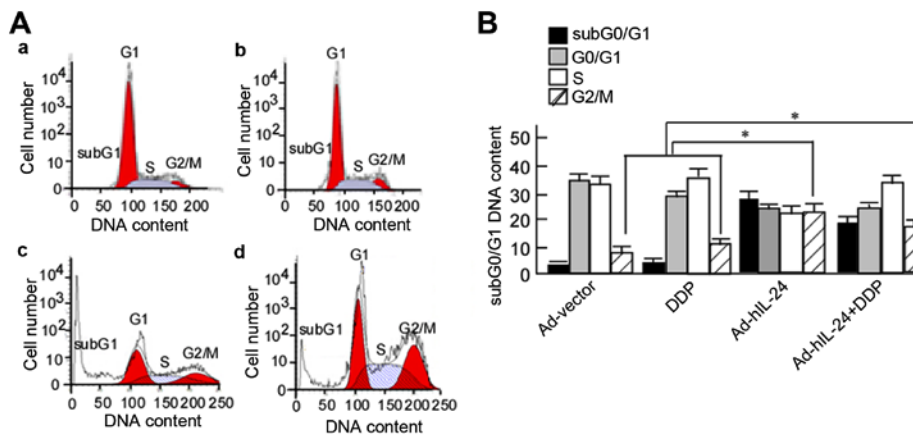


Figure 6. Cell cycle analysis of A549/DDP cells treated with Ad-hIL-24. A549/DDP cells were treated with DDP, Ad-hIL-24 and Ad-hIL-24 plus DDP, and then incubated for 48 h. The cells were harvested for flow cytometry. Ad-GFP was used as the vector control. (A) The cell cycle of treated cells was analyzed using flow cytometry. (B) Cells at the subG1, /G1, S and G2/M stages were assessed. Data are presented as the means  $\pm$  SD from three independent experiments statistically using the Student's t test ( $P < 0.05$ ).

expression, which induced cell-cycle arrest (25). The next step was to observe the cell cycle of A549/DDP cells. A549/DDP cells were treated with Ad-hIL-24, DDP, or Ad-hIL-24 plus DDP for 48 h, and the cell cycle distribution was analyzed using flow cytometry. The cells were arrested at the G2/M phase after being treated with hIL-24 (Fig. 6A-c and -d). The proportion of cells in the subG1, G1, S and G2/M phases was determined. G2/M-phase cells accounted for  $8.5\pm 1.32\%$ ,  $13.2\pm 2.14\%$ ,  $24.6\pm 4.33\%$ , and  $19.50\pm 4.12\%$  of cells in the Ad-vector, DDP, Ad-hIL-24, and DDP plus Ad-hIL-24 groups, respectively. Compared with the Ad-vector and DDP groups, the number of G2/M-phase cells was markedly increased in the Ad-hIL-24 and Ad-hIL-24 plus DDP groups (Fig. 6B,  $P<0.05$ ). This demonstrated that Ad-hIL-24 induced A549/DDP cell-cycle arrest.

## Discussion

The mortality and morbidity associated with lung cancer represent a serious threat to human health (26). Lung cancer patients often have an irritating cough, expectoration, hemoptysis, and other symptoms during the early stages of the disease, and its development is related to factors such as tumor location and pathological type (27). Lung cancer is divided into non-small cell and small cell lung cancer, with non-small cell lung cancer accounting for ~80% of all cases. Treatments for lung cancer are primarily based on the pathological type and the extent of local invasion and metastasis. In the early stages, treatment of lung cancer is predominantly surgical, while chemotherapy is an important alternative in the later stages (28). Platinum drugs alone or in combination with other drugs are considered the standard first-line chemotherapy agents for lung cancer treatment (29). The main mechanism of platinum drugs involves DNA recombination in tumor cells, which disrupts the structure and function of DNA and hinders DNA replication. These treatments exert anti-tumor effects, but also produce various side effects, including those affecting the digestive system, hematopoietic system and immune system in patients. Moreover, patients develop resistance to repeated chemotherapy, which decreases the survival rate (30). Reversing drug resistance and decreasing the toxic and side effects of chemotherapy drugs are two clinical concerns that must be addressed urgently.

The mechanism underlying tumor MDR is highly complex and involves many factors, although the overexpression of P-gp in tumor cells is one of the most important factors (31). To date, many studies have focused on the reversal of drug resistance in lung cancer, including the use of calcium channel blockers, anti-arrhythmia drugs and some traditional Chinese medicine components. Although certain drugs can momentarily increase chemotherapeutic drug concentrations to kill tumor cells, they cannot be widely used in a clinical setting because of their instability and non-specific nature, as well as the associated side effects. Therefore, it is essential to identifying more effective therapeutic strategies or drugs that can reverse lung cancer MDR and improve the survival rate of lung cancer patients.

Gene therapy is expected to provide a new therapeutic approach for decreasing drug resistance in cancer; this approach has the advantage of high selectivity and targeted inhibition of tumor cells. Currently, viral vectors are chiefly used for gene therapy. Adenoviral vectors share homology

with human genes and offer high levels of safety. In addition, adenoviral vectors are widely used due to their large capacity with respect to exogenous genes and range of hosts. Ad-hIL-24 was constructed with a recombinant adenoviral vector, and has been shown to exert an inhibitory effect on various tumors (32-34). Recently, Ad-hIL-24 was demonstrated to be capable of reversing tumor drug resistance. Ad-hIL-24 can not only induce cell apoptosis, but also reduce MDR gene expression (35,36). In the present study, we found that Ad-hIL-24 had a high rate of infection of lung cancer cells, and therefore may act as a suitable vector for tumor gene-therapy.

To investigate the drug-resistance-reversing effect of Ad-hIL-24, A549/DDP cells were used in this study. First, the inhibitory effect of Ad-hIL-24 on A549/DDP cells was detected. Ad-hIL-24 could significantly inhibit A549/DDP growth, and combining it with DDP enhanced this effect. This indicated that Ad-hIL-24 had an inhibitory effect on lung cancer cells that are resistant to DDP. We also observed that Ad-hIL-24 induced A549/DDP cell apoptosis. Based on the fluorescence microscopy findings, Ad-hIL-24 increased DDP-mediated A549/DDP cell apoptosis, and this was further confirmed by flow cytometric analysis. This suggests that Ad-hIL-24 has a reversal effect on the drug resistance of lung cancer and that it improves the sensitivity of lung cancer cells to DDP. Additionally, P-gp overexpression causes tumor cells to develop drug resistance. P-gp is a type of cell membrane protein, encoded by the MDR-1 gene (37), that can pump chemotherapeutic drugs out of cells, thereby decreasing the concentration of chemotherapeutic drugs inside cells and enhancing tumor cell resistance to these agents (38). We investigated whether hIL-24 could reverse the resistance of A549/DDP cells via altering the levels of P-gp, and found that Ad-hIL-24 significantly decreased P-gp expression. Ad-hIL-24 may decrease the activity of P-gp as a drug pump, enhancing the cytotoxic effect of DDP on A549/DDP cells, and eventually reverse the resistance of A549/DDP cells to DDP.

Akt is a key functional molecule of the PI3K/AKT signaling pathway, and p-AKT can resist antiapoptotic signals and promote cell apoptosis (39). In the current study, Ad-hIL-24 plus DDP decreased p-AKT expression, while the total Akt expression did not change significantly. Ad-hIL-24-mediated apoptosis may occur due to decreased Akt phosphorylation. A decrease in p-AKT expression induced cell apoptosis and arrested cells at the G2/M phase (24,25). Therefore, hIL-24 may reverse the resistance of A549/DDP cells through the induction of cell apoptosis and arresting cells at the G2/M phase. Additionally, IL-24 reversed the MDR of tumors through the PI3K/AKT signaling pathway (40-42), the double-stranded RNA-dependent protein kinase pathway, the Bcl-2 protein family (43), the mitochondrial pathway (44), and the endoplasmic reticulum stress pathway (45). Based on this, we speculated that Ad-hIL-24 may reverse A549/DDP cell resistance by affecting the PI3K/AKT signaling pathway. Further discussion is required and future experiments using the Rh123 method to assess the accumulation of chemotherapeutic drugs in drug-resistant tumor cells may help to elaborate the mechanism underlying the Ad-hIL-24-induced reversal of lung cancer MDR.

In summary, Ad-hIL-24 reversed the MDR of A549/DDP cells by inhibiting cell growth and inducing apoptosis. When

Ad-hIL-24 is combined with DDP, the reversal effect is enhanced compared with the single treatments. Regarding the mechanism, Ad-hIL-24 combined with DDP decreased P-gp expression, and its reversal effect may be through reducing the pumping of DDP out of the A549/DDP cells, thereby increasing DDP concentration in the cells. Ad-hIL-24 may also inhibit Akt phosphorylation and inhibit antiapoptotic signals to promote cell apoptosis and cell-cycle arrest at the G2/M phase, thus reversing tumor drug resistance.

### Acknowledgements

The authors acknowledge financial support from the National Natural Science Foundation of China (nos. 81372282, 81402368, 81402265 and 81502346), the Foundation of State Key Laboratory of Oncology in South China (HN2011-04), the Fundamental Research Funds for the Guangdong Province (2011B061300053), and the Zunyi Medical College Master Start Project (F-719).

### References

1. She J, Yang P, Hong Q and Bai C: Lung cancer in China: Challenges and interventions. *Chest* 143: 1117-1126, 2013.
2. Camps C, del Pozo N, Blasco A, Blasco P and Sirera R: Importance of quality of life in patients with non-small-cell lung cancer. *Clin Lung Cancer* 10: 83-90, 2009.
3. Satgé D, Kempf E, Dubois JB, Nishi M and Trédaniel J: Challenges in diagnosis and treatment of lung cancer in people with intellectual disabilities: Current state of knowledge. *Lung Cancer Int* 2016: 6787648, 2016.
4. Takase N, Hattori Y, Kiriu T, Itoh S, Kawa Y, Yamamoto M, Urata Y, Shimada T, Tsujino K, Soejima T, *et al*: Concurrent chemoradiotherapy with cisplatin and S-1 or vinorelbine for patients with stage III unresectable non-small cell lung cancer: A retrospective study. *Respir Investig* 54: 334-340, 2016.
5. Lunacek OE, Ravelo A, Coutinho AD, Hazard SJ, Green MR, Willey J, Eaddy M and Goertz HP: First-line treatment with bevacizumab and platinum doublet combination in non-squamous non-small cell lung cancer: A retrospective cohort study in US oncology community practices. *Drugs Real World Outcomes* 3: 333-343, 2016.
6. Teixeira SF, de Azevedo RA, Silva AC, Braga RC, Jorge SD, Barbutto JA, Andrade CH and Ferreira AK: Evaluation of cytotoxic effect of the combination of a pyridinyl carboxamide derivative and oxaliplatin on NCI-H1299 human non-small cell lung carcinoma cells. *Biomed Pharmacother* 84: 1019-1028, 2016.
7. Wu DL, Huang F and Lu HZ: Drug-resistant proteins in breast cancer: Recent progress in multidrug resistance. *Ai Zheng* 22: 441-444, 2003 (In Chinese).
8. Kim I, Xu W and Reed JC: Cell death and endoplasmic reticulum stress: Disease relevance and therapeutic opportunities. *Nat Rev Drug Discov* 7: 1013-1030, 2008.
9. Lage H: An overview of cancer multidrug resistance: A still unsolved problem. *Cell Mol Life Sci* 65: 3145-3167, 2008.
10. Joshi AA, Vaidya SS, St-Pierre MV, Mikheev AM, Desino KE, Nyandegde AN, Audus KL, Unadkat JD and Gerk PM: Placental ABC transporters: Biological impact and pharmaceutical significance. *Pharm Res* 33: 2847-2878, 2016.
11. Kong LL, Shen GL, Wang ZY, Zhuang XM, Xiao WB, Yuan M, Gong ZH and Li H: Inhibition of P-glycoprotein and multidrug resistance-associated protein 2 regulates the hepatobiliary excretion and plasma exposure of thienorphine and its glucuronide conjugate. *Front Pharmacol* 7: 242, 2016.
12. Wang NN, Zhao LJ, Wu LN, He MF, Qu JW, Zhao YB, Zhao WZ, Li JS and Wang JH: Mechanistic analysis of taxol-induced multidrug resistance in an ovarian cancer cell line. *Asian Pac J Cancer Prev* 14: 4983-4988, 2013.
13. Sourisseau T, Helissey C, Lefebvre C, Ponsonnailles F, Malka-Mahieu H, Olaussen KA, André F, Vagner S and Soria JC: Translational regulation of the mRNA encoding the ubiquitin peptidase USP1 involved in the DNA damage response as a determinant of Cisplatin resistance. *Cell Cycle* 15: 295-302, 2016.
14. Zuo J, Jiang H, Zhu YH, Wang YQ, Zhang W and Luan JJ: Regulation of MAPKs signaling contributes to the growth inhibition of 1,7-dihydroxy-3,4-dimethoxyxanthone on multidrug resistance A549/taxol cells. *Evid Based Complement Alternat Med* 2016: 2018704, 2016.
15. Mao Z, Bian G, Sheng W, He S, Yang J and Dong X: Adenovirus-mediated IL-24 expression enhances the chemosensitivity of multidrug-resistant gastric cancer cells to cisplatin. *Oncol Rep* 30: 2288-2296, 2013.
16. Dash R, Bhutia SK, Azab B, Su ZZ, Quinn BA, Kegelman TP, Das SK, Kim K, Lee SG, Park MA, *et al*: *mda-7/IL-24*: A unique member of the IL-10 gene family promoting cancer-targeted toxicity. *Cytokine Growth Factor Rev* 21: 381-391, 2010.
17. Liu J, Sheng W, Xie Y, Shan Y, Miao J, Xiang J and Yang J: The in vitro and in vivo antitumor activity of adenovirus-mediated interleukin-24 expression for laryngocarcinoma. *Cancer Biother Radiopharm* 25: 29-38, 2010.
18. Yu X, Xia W, Li S, Blumenfeld J, Zhang B, Yang J, Miao J and Gu ZJ: Antitumor effect and underlying mechanism of RGD-modified adenovirus mediated IL-24 expression on myeloid leukemia cells. *Int Immunopharmacol* 28: 560-570, 2015.
19. Chen F, Zhao Q, Wang S, Wang H and Li X: Upregulation of Id3 inhibits cell proliferation and induces apoptosis in A549/DDP human lung cancer cells in vitro. *Mol Med Rep* 14: 313-318, 2016.
20. Xie Y, Lv H, Sheng W, Miao J, Xiang J and Yang J: Synergistic tumor suppression by adenovirus-mediated inhibitor of growth 4 and interleukin-24 gene cotransfer in hepatocarcinoma cells. *Cancer Biother Radiopharm* 26: 681-695, 2011.
21. Zheng D, Chen Z, Chen J, Zhuang X, Feng J and Li J: Exogenous hydrogen sulfide exerts proliferation, anti-apoptosis, migration effects and accelerates cell cycle progression in multiple myeloma cells via activating the Akt pathway. *Oncol Rep* 36: 1909-1916, 2016.
22. Tang F, Zou F, Peng Z, Huang D, Wu Y, Chen Y, Duan C, Cao Y, Mei W, Tang X, *et al*: N,N'-dinitrosopiperazine-mediated ezrin protein phosphorylation via activation of Rho kinase and protein kinase C is involved in metastasis of nasopharyngeal carcinoma 6-10B cells. *J Biol Chem* 286: 36956-36967, 2011.
23. Kang T, Wei Y, Honaker Y, Yamaguchi H, Appella E, Hung MC and Piwnicka-Worms H: GSK-3 beta targets Cdc25A for ubiquitin-mediated proteolysis, and GSK-3 beta inactivation correlates with Cdc25A overproduction in human cancers. *Cancer Cell* 13: 36-47, 2008.
24. Xiao M, Tang Y, Wang YL, Yang L, Li X, Kuang J and Song GL: ART1 silencing enhances apoptosis of mouse CT26 cells via the PI3K/Akt/NF- $\kappa$ B pathway. *Cell Physiol Biochem* 32: 1587-1599, 2013.
25. Li Y, Zhang P, Qiu F, Chen L, Miao C, Li J, Xiao W and Ma E: Inactivation of PI3K/Akt signaling mediates proliferation inhibition and G2/M phase arrest induced by andrographolide in human glioblastoma cells. *Life Sci* 90: 962-967, 2012.
26. Chen W, Zhang S and Zou X: Evaluation on the incidence, mortality and tendency of lung cancer in China. *Thorac Cancer* 1: 35-40, 2010.
27. Lee PN and Gosney JR: The effect of time changes in diagnosing lung cancer type on its recorded distribution, with particular reference to adenocarcinoma. *Regul Toxicol Pharmacol* 81: 322-333, 2016.
28. Mak KS, van Bommel AC, Stowell C, Abrahm JL, Baker M, Baldotto CS, Baldwin DR, Borthwick D, Carbone DP, Chen AB, *et al*: Lung Cancer Working Group of ICHOM: Defining a standard set of patient-centred outcomes for lung cancer. *Eur Respir J* 48: 852-860, 2016.
29. Yamada K, Ichiki M, Takahashi K, Hisamatsu Y, Takeoka H, Azuma K, Shukuya T, Nishikawa K, Tokito T, Ishii H, *et al*: A multicenter phase II trial of S-1 combined with bevacizumab after platinum-based chemotherapy in patients with advanced non-squamous non-small cell lung cancer. *Cancer Chemother Pharmacol* 78: 501-507, 2016.
30. Darwish MA, Abo-Youssef AM, Khalaf MM, Abo-Saif AA, Saleh IG and Abdelghany TM: Vitamin E mitigates cisplatin-induced nephrotoxicity due to reversal of oxidative/nitrosative stress, suppression of inflammation and reduction of total renal platinum accumulation. *J Biochem Mol Toxicol* 31: 1-9, 2017.
31. Takara K, Sakaeda T, Kakumoto M, Tanigawara Y, Kobayashi H, Okumura K, Ohnishi N and Yokoyama T: Effects of alpha-adrenoceptor antagonist doxazosin on MDR1-mediated multidrug resistance and transcellular transport. *Oncol Res* 17: 527-533, 2009.



32. Pan XT, Zhu QY, Li DC, Yang JC, Zhang ZX, Zhu XG and Zhao H: Effect of recombinant adenovirus vector mediated human interleukin-24 gene transfection on pancreatic carcinoma growth. *Chin Med J* 121: 2031-2036, 2008.
33. Zheng SY, Ge JF, Zhao J, Jiang D and Li F: Adenovirus-mediated IL-24 confers radiosensitization to human lung adenocarcinoma in vitro and in vivo. *Mol Biol Rep* 42: 1069-1080, 2015.
34. Lv C, Su Q, Liang Y, Hu J and Yuan S: Oncolytic vaccine virus harbouring the IL-24 gene suppresses the growth of lung cancer by inducing apoptosis. *Biochem Biophys Res Commun* 476: 21-28, 2016.
35. Xu J, Mo Y, Wang X, Liu J, Zhang X, Wang J, Hu L, Yang C, Chen L and Wang Y: Conditionally replicative adenovirus-based mda-7/IL-24 expression enhances sensitivity of colon cancer cells to 5-fluorouracil and doxorubicin. *J Gastroenterol* 48: 203-213, 2013.
36. Fang P, Zhang X, Gao Y, Ding CR, Cui F and Jiao SC: Reversal effect of melanoma differentiation associated gene-7/interleukin-24 on multidrug resistance in human hepatocellular carcinoma cells. *Anat Rec* 295: 1639-1646, 2012.
37. Bajaj G, Rodriguez-Proteau R, Venkataraman A, Fan Y, Kioussi C and Ishmael JE: MDR1 function is sensitive to the phosphorylation state of myosin regulatory light chain. *Biochem Biophys Res Commun* 398: 7-12, 2010.
38. Yun UJ, Lee JH, Koo KH, Ye SK, Kim SY, Lee CH and Kim YN: Lipid raft modulation by Rpl reverses multidrug resistance via inactivating MDR-1 and Src inhibition. *Biochem Pharmacol* 85: 1441-1453, 2013.
39. Yu XS, Du J, Fan YJ, Liu FJ, Cao LL, Liang N, Xu DG and Zhang JD: Activation of endoplasmic reticulum stress promotes autophagy and apoptosis and reverses chemoresistance of human small cell lung cancer cells by inhibiting the PI3K/AKT/mTOR signaling pathway. *Oncotarget* 7: 76827-76839, 2016.
40. Burris HA III: Overcoming acquired resistance to anticancer therapy: Focus on the PI3K/AKT/mTOR pathway. *Cancer Chemother Pharmacol* 71: 829-842, 2013.
41. Mosca E, Barcella M, Alfieri R, Bevilacqua A, Canti G and Milanesi L: Systems biology of the metabolic network regulated by the Akt pathway. *Biotechnol Adv* 30: 131-141, 2012.
42. Polivka J Jr and Janku F: Molecular targets for cancer therapy in the PI3K/AKT/mTOR pathway. *Pharmacol Ther* 142: 164-175, 2014.
43. Pataer A, Chada S, Roth JA, Hunt KK and Swisher SG: Development of Ad-mda7/IL-24-resistant lung cancer cell lines. *Cancer Biol Ther* 7: 103-108, 2008.
44. Yang BX, Duan YJ, Dong CY, Zhang F, Gao WF, Cui XY, Lin YM and Ma XT: Novel functions for *mda-7/IL-24* and *IL-24 delE5*: Regulation of differentiation of acute myeloid leukemic cells. *Mol Cancer Ther* 10: 615-625, 2011.
45. Shi H, Wei LL, Yuan CF, Yang JX, Yi FP, Ma YP and Song FZ: Melanoma differentiation-associated gene-7/interleukin 24 inhibits invasion and migration of human cervical cancer cells in vitro. *Saudi Med J* 28: 1671-1675, 2007.